Axisymmetric finite volumes for the numerical simulation of bulk CO_2 transport and assimilation in a leaf

Emily Gallouët[†]

[†]*ENS, 45 rue d'Ulm, 75005 Paris, France*

emily.gallouet@ens.fr

Raphaèle Herbin[⋆]

[⋆]*LATP, Université de Provence, 33 rue Joliot Curie, 13453 Marseille, France*

herbin@cmi.univ-mrs.fr

Abstract

This paper deals with the numerical simulation of CO_2 transport in the leaf. We study a mathematical model of the diffusion and photosynthesis processes, and present the implementation of an axisymmetric cell centred finite volume scheme for their numerical simulation. The resulting code enables the computation of the lateral diffusion coefficient in the leaf porous medium, from experimental measurements which yield the point wise value of internal CO_2 concentration. Hence our model and numerical code allow the analysis of the role of the internal diffusion in the photosynthesis process. We show here that under moderate light, CO_2 does not diffuse across long distances because it is rapidly assimilated by photosynthesising cells.

Key words : CO_2 diffusion, photosynthesis, porous medium, finite volumes.

1 Introduction

The object of the present work is to develop a mathematical model to describe and quantify the diffusion phenomena within the leaf tissue. Indeed, this model felt needed after a series of experiences involving fluorescence measurements of the internal CO_2 concentration within the leaf tissue was set up at Essex University [7, 12]. In fact, CO_2 diffusion within the leaf tissue is a crucial process in the photosynthetic activity of plants. Once the CO_2 enters the leaf tissues through stomata, (the stomata are spaces of the leaf surface through wich exchange with the atmosphere takes place), it diffuses towards the photosynthetic cells in the so-called intercellular air space (IAS). Since the stomata are usually uniformly distributed across the leaf surface, vertical CO_2 diffusion seems to be more important than lateral diffusion. However, in stress

situations, plants tend to close their stomata in patches; hence the question of the role of lateral diffusion in these situations, where the photosynthetic cells may be away from open stomata. One of the goal of the experience and the associated mathematical model was to analyse the role of lateral diffusion in such cases. Other diffusion models have been developed, but at the stomatal scale. For instance, in [1], the 3D diffusion is modelled at the scale of a single stoma in Scots pine needles. In [14], a 2D finite element model is constructed to assess the influence of the stomatal density on photosynthesis and transpiration. Here we are more interested in lateral diffusion at a larger scale, and will therefore model the leaf tissue as a porous media.

The resulting mathematical model which describes the biological phenomena under consideration is a semi-linear diffusion equation (the nonlinearity arises in the assimilation function of the photosynthesis) with mixed Neumann and Robin boundary conditions. We choose to discretize the equation with the finite volume method (rather than the finite element method) because it involves a direct discretization of the fluxes at interfaces which are of crucial importance here, and it is well adapted to the axisymmetric geometry under consideration. The numerical analysis of the cell-centred finite volume (FV) method for diffusion problems is now well-known. In the case of semi linear equations with Dirichlet boundary conditions, the convergence of the FV scheme is shown in [4]. In the case of Robin conditions such as considered here, an error estimate was obtained for linear convection-diffusion–reaction problems in [8]. In the present case, we are able to discretize the geometry in such a way that the consistency of the discretized inner fluxes is of order 2. Since the resulting discrete system is nonlinear, we adopt a monotony method to solve it in a robust way.

We emphasise that the present model allows the estimation (from experimental data) of a Lateral diffusion coefficient of the porous media and the determination of the relative contribution of anatomy and sink strength in restricting CO_2 diffusion. This quantitative analysis yields a better understanding of the leaf physiology.

The paper is organised as follows: in Section 2, we describe the biological problem and the experiences that were performed to measure the CO_2 diffusion under the patch. The mathematical model, based upon a diffusion equation for the transport of CO_2 and a kinetic-type relation between assimilation and CO_2 internal molar fraction is presented in Section 3. It is proven that the resulting semi linear diffusion equation with Robin boundary conditions is well posed, in the sense that its weak solution exists, is unique, and satisfies the physical bounds. Section 4 is devoted to the discretization of the the diffusion equation by an axisymmetric finite volume scheme. The resulting discrete system of equations is also shown to be well posed (existence, uniqueness, and physical bounds). Convergence of the approximate solution towards the weak solution is obtained when the mesh is refined. In Section 5 we briefly present the monotony method which is used for the resolution of the nonlinear system. Section 6 is then devoted to the determination of the diffusion parameter D_{CO_2} from the experimental results and the mathematical model. We conclude by a number of perspectives that this work leads to.

2 Biological problem and experimental data

Green plants are able to use energy from light to synthesise their own carbohydrates, $[CH_2O]n$, from soil water (H_2O) and atmospheric carbon dioxide (CO_2). This essential process, called photosynthesis, can be summarised by the general equation: $n(CO_2 + H_20) +$ light energy $\rightarrow$ $[CH_2O]n + nO_2$. Photosynthesis takes place in the so called mesophyll, which consists of sev-

eral layers and makes up most of the leaf interior. The mesophyll is surrounded by epidermal cells covered with an impermeable cuticle. Consequently exchanges between the leaf and the atmosphere take place exclusively through "pores" called stomata whose aperture may vary. Atmospheric CO_2 diffuses through the stomata into the leaf. It then diffuses in the inter cellular airspace, made from the gap between cells, to reach the photosynthesising cells where it is assimilated. There are essentially two important fluxes taking place through the stomata: a flux of CO_2 from the atmosphere into the leaf and a flux of H_2O from the leaf to the atmosphere. Stomatal aperture constantly adjusts to the external and internal conditions to maximise the photosynthetic rate and minimise H_2O evaporation. Under dry conditions for instance stomata tend to close. In some cases stomatal aperture is heterogeneous across the leaf surface [10]. Groups of closed stomata can be next to groups of open stomata. It has been shown that such behaviour, referred to as "patchy stomatal closure", can lead to heterogeneous photosynthesis across the leaf due to heterogeneous CO_2 supply in the mesophyll [18]. Indeed, variations in internal CO_2 molar fraction have an important influence on the carbon assimilation rate and thus on the production of carbohydrates by the leaf [3]. In C_3 plants, the first essential step in the synthesis of carbohydrates is the carboxylation : the CO_2 is attached to an acceptor, made of a skeleton of 5 carbons, which produces two molecules of 3 carbons each. This reaction is catalysed by the enzyme Rubisco which is very sensitive to variation in CO_2 molar fraction around ambient molar fraction ($380ppm$): this will lead to a non linearity in the mathematical model. In this study we are interested in CO_2 diffusion in the intercellular air space. Indeed we wish to understand the extent to which intercellular diffusion may compensate patchy stomatal behaviour. In other words, can cells under a group of closed stomata still maintain high photosynthetic rate thanks to the CO_2 supply from lateral diffusion? Moreover there are two major factors determining internal diffusion: physical resistance to diffusion, linked to the anatomy of the leaf, and sink strength (photosynthesising cells consuming CO_2 along the path). It is crucial to quantify the relative contribution of these two factors in limiting CO_2 diffusion in order to better understand the plant physiology.

To address these questions, experiments were performed by the first author at the Department of Biological Sciences at the University of Essex [12] on *Phaseolus vulgaris* (the common bean) a C_3 plant. Groups of stomata were artificially blocked by applying circular patches of silicon grease ($4mm$ diameter) symetrically on both surfaces of the leaf. For the patched area diffusion through the stomata is suppressed, consequently the supply of CO_2 under the patch solely comes from lateral diffusion from the surrounding tissues. Combined infrared gas analysis and chlorophyll a fluorescence imaging was then used to map CO_2 molar fraction in the leaves to a high resolution [11].

2.1 Experimental results

Figure 2.1 represents a typical experimental result. It shows a map of the internal CO_2 molar fraction c for a $6mm$ wide square portion of a leaf. The z axis gives c in ppm. The circular patch of grease ($4mm$ diameter), which artificially prevents exchanges with the atmosphere, is at the center of the plot. The x and y axes give the distance of a point from the center of the patch. Atmospheric CO_2 (c_a) is free to penetrate the leaf, through the stomata, outside the patch area. In this example c_a is set at $364ppm$, a little below the natural molar fraction. We can clearly visualise a steep c gradient from the outside of the patch, where c is quite homogeneous, to the center of the patch. It is worth noting that these images are obtained a few minutes
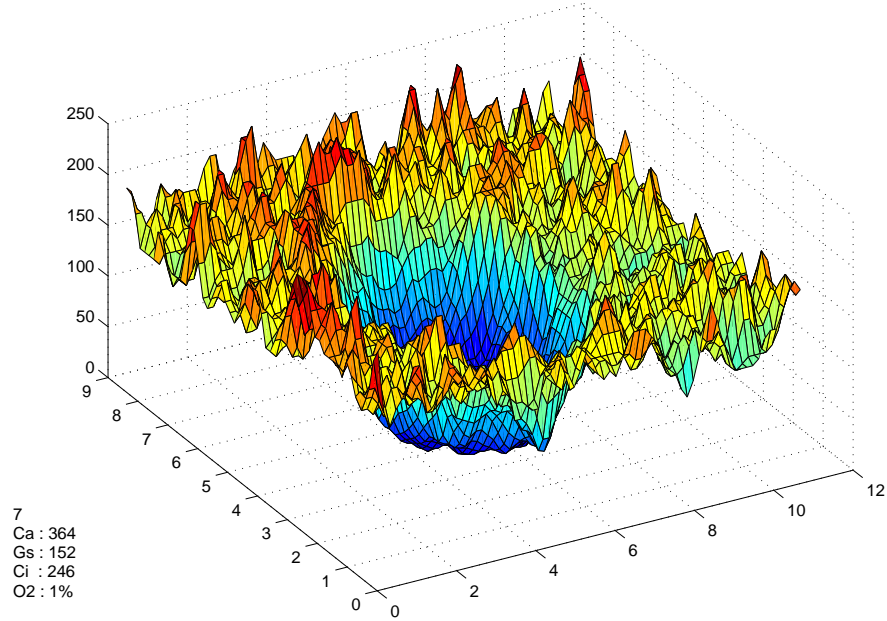
Figure 1: Map of intercellular CO_2 molar fraction (x, y axis : mm, z axis : c in ppm. Ca : external CO_2 molar fraction (ppm), Gs : stomatal conductance ($mmol$ m^{-2} s^{-1}) and Ci mean Internal CO_2 molar fraction outside the patch given by gas exchanges measurements. O_2 : % oxygen in the air.)

after the patch has been applied to allow for the steady state to be reached. We can already conclude that CO_2 from the tissues surrounding the patch is unable to give a sufficient supply to photosynthesising cells under the patch. However at this stage we cannot go further in the analysis: why does the CO_2 not diffuse well? Is it due to cell packing and physical limitation of the internal diffusion? or is the CO_2 consumed so rapidly that it is simply not available to distant cells?

We need a tool to quantify these phenomena and distinguish between the two factors. Whether the anatomical or the biochemical limitation is greater will lead to a different interpretation of the leaf behaviour with regards to stomatal regulation and internal anatomy. Measurements similar to the example shown here were conducted at different external CO_2 molar fractions (c_a), from $50ppm$ to $2000ppm$. This variety of measures helps us to characterise the phenomenon and gives a good material to build and validate a mathematical model.

2.2 Diffusion pathway and scale of measurements

The flux of CO_2 through stomatal pores ($J^s_{CO_2}$ in mol m^{-2} s^{-1}) can be described by Fick's first law in the following way [13]:

$$J^s_{CO_2} = D^{fa}_{CO_2} \times \frac{\delta CO_2}{\delta x}$$

where $D^{fa}_{CO_2}$ is the diffusion coefficient of CO_2 in free air (in mol m^{-1} s^{-1}) and δCO_2 the difference in CO_2 molar fraction (ppm) across δx, the mean distance (in m) travelled by the

molecules from still air through the boundary layer and the pore depth, to the intercellular air spaces. In the species studied, stomata are present on both the lower and upper surface with a density of 100 $stomata\ mm^{-2}$ on the lower and 20 $stomata\ mm^{-2}$ on the upper surface. measurements of c are performed on square leaf portions of encompassing approximately 2 stomata [12]. Therefore we study the phenomenon at a macroscopic scale considering the stomata to be evenly open and distributed at the surface of the leaf outside the artificially patched area. The CO_2 flux per unit surface of the leaf ($J_{CO_2}^l$)becomes:

$$J_{CO_2}^l = D_{CO_2}^{fa} \frac{\delta CO_2}{\delta x} \times \frac{S_{st}}{S}$$

where S_{st} is the open stomatal area on the leaf area S. The stomatal conductance, g_s, is defined as $D_{CO_2}^{fa} \times \frac{S_{st}}{\delta x \times S}$. This parameter can be measured experimentally, by gaz exchanges, for a large surface ($10cm^2$). It varies with S_{st} which is directly linked to stomatal aperture. For each map of CO_2 we also measured gs (outside the patch) by the gaz exchange method.

2.3   Assimilation rate and intercellular molar fraction

The assimilation rate A is linked to the intercellular molar fraction c which may be determined from gas exchange measurements. The equation used to describe this relation is derived from the chemical properties of the carboxylation enzyme Rubisco.
The assimilation rate A is linked to the intercellular molar fraction c. The equation used describe this relation is derived from the chemical properties of the carboxylation enzyme Rubisco. Under non-photorespiratory condition and constant light it takes the following Michaelis-Menten form (adapted from [6]):

$$A(c,z) = \frac{V_{c_{max}}(z)c}{c + K_c(z)} - R_d(z), \tag{1}$$

where $V_{c_{max}}(z)$ is the maximal assimilation velocity ($mol\ m^{-3}\ s^{-1}$), $K_c(z)$ the Michaelis constant (ppm) and $R_d(z)$ the respiration rate ($mol\ m^{-3}\ s-1$) at depth z inside the leaf. Note that even in the light the plant respires, which is a source of CO_2 inside the leaf, hence the term R_d. At the point where c becomes non limiting this relation breaks into $A = A_{max}(z)$ Under the experimental conditions considered here, the $A - c, z$ relation is described by the following formula:

$$A(c,z) = \begin{cases} \min(A_{max}(z), \frac{V_{c_{max}}(z)c}{c+K_c(z)} - R_d(z)) \text{ if } c > 0, \\ A(c,z) = -R_d(z) \text{ otherwise,} \end{cases} \tag{2}$$

At the so called compensation point

$$c_z^* = \frac{R_d(z) \times K_c(z)}{V_{cmax}(z) - R_d(z)}, \tag{3}$$

the carboxylation rate $\kappa = \frac{V_{cmax}c}{c+K_c}$ is equal to the respiration rate R_d, so the net CO_2 assimilation is zero. During experimentation the external CO_2 molar fraction c_a has always been maintained above c_z^*, and therefore, during the experience, the intercellular molar fraction c stays above c^*. We shall prove in Theorem 3.2 below that under the above experimental conditions the molar fractions given by the mathematical model also satisfy $c \geq c_z^*$.

In the experiments presented in this paper we did not detailed the z variations. We Measured A at different c for a leaf surface area using classical gaz exchange method. This yields yields to an empirical $A-c$ relation for the entire thickness of the leaf, the theoretical relation is then derived from these experimental curves. we work under non-photorespiratory conditions ($1\%O_2$in the air used) and constant light (Photon Flux Density of 400 $\mu mol.m^{-2}.s^{-1}$) The respiration rate is assumed to be constant, here it is about 6 times smaller than maximal assimilation rate. There is a good correlation between the experimental data and the theoretical relation fitted using simplified Eq.(1) (without the z dependency) : the correlation coefficient between the two curves is greater than 0.98.

3   The mathematical model

The physical domain $\Omega = \{(r, \theta, z), 0 \leq r \leq R, 0 \leq \theta \leq 2\pi, 0 \leq z \leq H\}$ is depicted in Figure 2. It consists in a cylindrical section of a leaf, the thickness of which is denoted by H. The axis of the cylinder runs through the center point of the patches, which are located symmetrically on both lower (Σ_ℓ) and upper (Σ_u) surfaces of the leaf. The radius R of this cylinder is chosen large enough so that the diffusion flux on its lateral side is negligible. We use cylindrical coordinates r, z, θ to describe the area of study. Let $\partial\Omega$ denote the boundary of Ω. One has $\partial\Omega = \Sigma_R \cup \Sigma_u \cup \Sigma_\ell$, where $\Sigma_R = \{(R, z, \theta), 0 \leq z \leq H, 0 \leq \theta \leq 2\pi\}$ is the lateral boundary of Ω, $\Sigma_u = \{(r, H, \theta), 0 \leq r \leq R, 0 \leq \theta \leq 2\pi\}$ (resp. $\Sigma_\ell = \{(r, 0, \theta), 0 \leq r \leq R, 0 \leq \theta \leq 2\pi\}$) is the upper (resp. lower) surface. The blue area describes the patches $\Sigma_P = \{(r, z, \theta), 0 \leq r \leq R_P, z = 0 \text{ or } z = h, 0 \leq \theta \leq 2\pi\}$. The anatomy of the leaf (see e.g. [13]) is such that, at sufficiently large scale, it may be considered as a porous media, with permeability depending only on z. For the problem under consideration, we may therefore assume the CO_2 molar fraction to be constant in the θ dimension, and consider the problem to be axisymmetric. The diffusion coefficient D_{CO_2} of the porous media of the leaf is unknown. In the sequel, for the sake of simplicity of notations, we shall denote it by D. One of the goals of the mathematical model is to determine its value from the above experimental data. In order to do so, let us first establish the mathematical equations which rule the internal concentration c.

DEFINITION 3.1 (Properties of the nonlinear sink term) Let A be the assimilation of CO_2 by photosynthesis, defined by (2), and let f be defined as

$$f(c, x) = -A(c, z) = \begin{cases} \max\left(-A_{max}(z), R_d(z) - \frac{V_{cmax}(z)\, c}{c + K_c(z)}\right) & \text{if } c > 0, \\ A(c, z) = R_d(z) & \text{otherwise} \end{cases} \quad \forall\, c \in \mathbb{R}, \quad (4)$$

Therefore, f is a bounded decreasing function of c.

The diffusion equation for CO_2 (see [13]) reads:

$$-\nabla \cdot (D\nabla c) = f(c, .) \text{ in } \Omega, \tag{5}$$

(recall that $D = D_{CO_2}$) with homogeneous Neumann boundary conditions on the lateral side of Ω :

$$-D\nabla c \cdot \mathbf{n} = 0, \text{ on } \Sigma_R \tag{6}$$

and Robin conditions due to the incoming flux of CO_2 through the stomata of the leaf :

$$-D\nabla c \cdot \mathbf{n} = fl_{st} = g_s(c_a - c), \text{ on } \Sigma_u \cup \Sigma_\ell, \tag{7}$$

where g_s is the stomatal conductance defined in the previous section, which we set to 0 on Σ_P, since the stomata are blocked by the patch, and c_a is the atmospheric CO_2 concentration. Since c_a is assumed to be higher than the compensation point c_z^* defined by (3), for which f changes sign. Hence the function f satisfies:

(i) if $c \leq c_z^*$ then $f(c, z) \geq 0$.

(ii) if $c \geq c_a$ then $f(c, z) \leq 0$.

Note that for the leaf considered as a porous medium, if the direction z is perpendicular to the surface of the leaf, then the coefficient matrix D is of the form:

$$D = \begin{pmatrix} d_r & 0 & 0 \\ 0 & d_r & 0 \\ 0 & 0 & d_z \end{pmatrix}, \tag{8}$$

where d_r, the "horizontal" diffusion coefficient (resp. d_z, the vertical diffusion coefficient) only depends on the coordinate in the z direction, and is bounded by below by a positive constant. The problem (5)–(7) is well posed, in the sense that there exists a unique (and non negative) solution of the weak formulation of (5)–(7) in an adequate functional space, as stated below. Furthermore, this solution satisfies the physical bounds $c_z^* \leq c \leq c_a$.

THEOREM 3.2 (WELL POSEDNESS) Let f be defined by (4), $g_s > 0$ and $c_a \geq c_z^*$, where c_z^* is the compensation point defined by (3), let D be defined by (8), then there exists a unique function $c \in H^1(\Omega)$ such that:

$$\begin{cases} c \in H^1(\Omega), \\ \displaystyle\int_\Omega D(x)\nabla c(x) \cdot \nabla\varphi(x)dx + \int_{\Sigma_U \cup \Sigma_R} g_s(c(x) - c_a)\varphi(x)d\gamma(x) = \int_\Omega f(c(x), x)\varphi(x)dx, \\ \hspace{9cm} \forall\varphi \in H^1(\Omega). \end{cases} \tag{9}$$

where dx is the integration symbol for an open bounded set of $\mathbb{R}^3$ and $d\gamma(x)$ the integration symbol for a surface of $\mathbb{R}^2$. Moreover,

$$c_z^* \leq c \leq c_a \text{ a.e. in } \Omega.$$

Proof The existence of c is a consequence of Schauder's fixed point theorem [2], which may be applied to the fixed point operator T defined by $c = T(\widetilde{c})$, where c is the unique function (by the Lax Milgram theorem) such that:

$$\begin{cases} c \in H^1(\Omega), \\ \displaystyle\int_\Omega D(x)\nabla c(x) \cdot \nabla\varphi(x) \, dx + \int_{\Sigma_U \cup \Sigma_R} g_s(c(x) - c_a)\varphi(x) \, d\gamma(x) = \int_\Omega f(\widetilde{c}(x), x)\varphi(x) \, dx, \\ \hspace{9cm} \forall\varphi \in H^1(\Omega). \end{cases} \tag{10}$$

Indeed, T is compact as an operator from $L^2(\Omega)$ in in $L^2(\Omega)$, thanks to the fact that f is bounded.

Uniqueness is easily obtained by taking $\varphi = c_1 - c_2$ in (9), where c_1 and c_2 are two potential solutions of (9), and using the fact that f is decreasing.

Finally, one proves that $c \leq c_a$ by taking $\varphi = (c - c_a)^+ (= \max(0, c - c_a))$ in (9) and using the fact that f is non-positive if $c \geq c_a$ (see Definition 3.1). Similarly, one proves that $c \geq c_z^*$ by taking $\varphi = (c - c_z^*)^- (= -\min(0, c - c_z^*))$ in (9) and using the fact that $f \geq 0$ if $c \leq c_z^*$.

$\square$

4 The axisymmetric finite volume scheme

Assume that we know the diffusion parameter D, and we wish to find an approximate solution c of Problem (5)–(7). In order to compute an approximate solution, we first discretize the diffusion equation by an axisymmetric finite volume scheme. The finite volume strategy is very well adapted to the axisymmetric geometry, and in particular, much more so than the usual finite difference scheme on the Laplace operator written in cylindrical coordinates, where a term in $\frac{1}{r}$ appears, which can yield a bad condition number for the resulting discretization matrix.

DEFINITION 4.1 (Axisymmetric finite volume mesh) Let $N_r \in \mathbb{N}$, $N_z \in \mathbb{N}$, and let $(r_i)_{i=0,\ldots N_r} \subset [0, R]$ and $(z_j)_{j=0,\ldots N_z} \in [0, H]$ such that $r_1 = 0 < r_2 < \cdots < r_i < r_{i+1} \cdots < r_{N_r} < R$, and $0 < z_1 < z_2 < \cdots < z_j < z_{j+1} \cdots < r_{N_z} < H$. We choose the values r_i such that there exists a radial interface corresponding to the patch, that is, there exists $i_P \in \{1, \ldots, N_r - 1\}$ such that $r_{i_P+1/2} = R_P$, where the values $r_{i+1/2}$ are defined by:

$$r_{i+1/2} = \frac{r_i + r_{i+1}}{2} \text{ for } i = 1, \ldots, N_r - 1, \text{ and } r_{N_r+1/2} = R,$$

and similarly:

$$z_{1/2} = 0, \ z_{j+1/2} = \frac{z_j + z_{j+1}}{2} for \text{ for } j = 1, \ldots, N_z - 1, \text{ and } z_{N_z+1/2} = H,$$

The physical domain Ω defined in the previous section is discretized in $N = (N_r + 1) \times N_z$ annular control volumes defined by

$$K_{0,j} = \{(r, z, \theta), 0 \le r < r_{3/2}, z_{j-1/2} \le z < z_{j+1/2}, 0 \le \theta \le 2\pi\}, j = 1, \ldots, N_z,$$
$$K_{i,j} = \{(r, z, \theta), r_{i-1/2} \le r < r_{i+1/2}, z_{j-1/2} \le z < z_{j+1/2}, 0 \le \theta \le 2\pi\}, \left\{ \begin{array}{l} i = 1, \ldots, N_r, \\ j = 1, \ldots, N_z. \end{array} \right.$$

The mesh $\mathcal{M}$ is defined as the set of control volumes, i.e.

$$\mathcal{M} = (K_{i,j})_{\substack{i=1,\ldots,N_r \\ j=1,\ldots,N_z}},$$

and by $h_{\mathcal{M}}$ the size of the mesh, that is:

$$h_{\mathcal{M}} = \max\left(\max\{\rho_i\}, i = 1, \ldots, N_r\}, \max\{h_j, j = 1, \ldots, N_z\}\right),$$

where $\rho_i = r_{i+1/2} - r_{i-1/2}$ for $i = 2, \ldots, N_r$, $\rho_1 = 2r_{3/2}$, and $h_j = z_{i+1/2} - z_{i-1/2}$ for $j = 1, \ldots N_z$.

Let us emphasise that the above defined mesh satisfies the orthogonality condition given in Definition 9.1 of [5]. This condition is crucial for the consistency of the fluxes, and indeed, the proofs of convergence and error estimates may be adapted for this kind of mesh. Furthermore, with the above choice of interfaces, we have order 2 consistency of the internal fluxes. Let us also note that the compatibility of the boundary of a control volume with the boundary of a patch is not necessary to define the scheme, nor to prove its convergence. This choice was made because of implementation and visualisation considerations.

In order to obtain the finite volume scheme, the diffusion equation (5) is integrated over each control volume. Using the Stokes formula, this leads to the following flux balance equation:
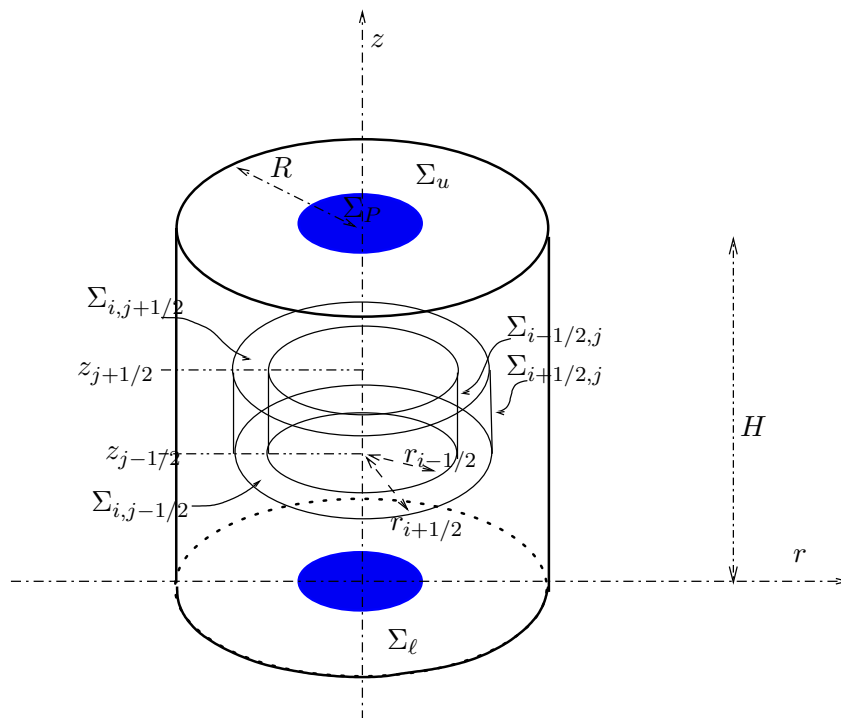
Figure 2: The physical domain (thick lines) of the model: a cylindrical portion of the leaf, (the blue area represents the patch) and a control volume $K_{i,j}$ (thin line) for flux balance

$$\int_{\partial K_{i,j}} -D(x)\nabla c(x) \cdot \mathbf{n}(x)d\gamma(x) = \int_{K_{i,j}} f(c(x),x)dx. \tag{11}$$

We decompose $\partial K_{i,j} = \Sigma_{i-1/2,j} \cup \Sigma_{i+1/2,j} \cup \Sigma_{i,j-1/2} \cup \Sigma_{i,j+1/2}$ as shown on Figure 2, and write (11) as:

$$\mathcal{F}_{i-1/2,j} + \mathcal{F}_{i+1/2,j} + \mathcal{F}_{i,j+1/2} + \mathcal{F}_{i,j-1/2} = \int_{K_{i,j}} f(c(x),x)dx,$$

where $\mathcal{F}_{i,j+1/2}$ denotes the diffusion flux through the surface $\Sigma_{i,j+1/2}$ outward to $K_{i,j}$. Let us now introduce the discrete unknowns $(c_{i,j})_{\substack{i=1,\dots,N_r \\ j=1,\dots,N_z}}$, associated to the control volumes $K_{i,j}$, and which are expected to be approximate values of c inside the control volumes $K_{i,j}$; denote by $(F_{i+1/2,j})_{\substack{i=0,\dots N_r \\ j=0,\dots N_z}}$ (resp. $(F_{i,j+1/2})_{\substack{i=0,\dots N_r \\ j=0,\dots N_z}}$) the radial interface (resp. horizontal interface) numerical fluxes, which are expected to be approximations of the real fluxes $\mathcal{F}_{i+1/2,j}$ (resp. $\mathcal{F}_{i,j+1/2}$) through the boundaries of the control volume $K_{i,j}$. An approximate equation to (11) is now:

$$F_{i-1/2,j-1/2} + F_{i+1/2,j-1/2} + F_{i-1/2,j+1/2} + F_{i+1/2,j+1/2} = |K_{i,j}|f(c_{i,j}), \tag{12}$$

where $|K_{i,j}|$ denotes the volume of $K_{i,j}$. In order to fully define the finite volume scheme, we need to express the numerical fluxes $F_{i,j}$ in terms of the discrete unknowns $c_{i,j}$. This expression depends on the interface through which the flux $\mathcal{F}_{i,j}$ is defined. On internal faces, an easy discretization of the normal gradient is obtained by a centred finite difference scheme. On

external faces, the boundary conditions (null flux under the patch and on the lateral boundaries, Robin condition on the upper and lower surfaces outside the patch) are taken into account. We thus obtain the following expressions (note that the diffusion coefficients d_r and d_z depend on z only):

- Lateral internal interfaces:

$$F_{i+1/2,j} = d_{r,i+1/2} |\Sigma_{i+1/2,j}| \frac{c_{i+1} - c_i}{r_{i+1} - r_i}, \ i = 0, \ldots, N_r - 1, \ j = 1, \ldots, N_z. \tag{13}$$

- Horizontal internal interfaces:

$$F_{i,j+1/2} = d_{z,j+1/2} |\Sigma_{i,j+1/2}| \frac{c_{j+1} - c_j}{z_{j+1} - z_i}, \ i = 0, \ldots, N_r, \ j = 0, \ldots, N_z. \tag{14}$$

- Lateral boundary interfaces:

$$F_{N_r+1/2,j} = 0, \ j = 1, \ldots, N_z. \tag{15}$$

- Horizontal boundary interfaces:

  - interface outside the patch, for $i \geq i_P$:

$$
\begin{aligned}
F_{i,1/2} &= |\Sigma_{i,1/2}| \frac{2d_{z,1/2}g_s}{2z_1 g_s + 2d_{z,1/2}} (c_{i,1} - c_a), \\
F_{i,N_z+1/2} &= |\Sigma_{i,N_z+1/2}| \frac{2d_{z,N_z+1/2}g_s}{2(H - z_N)g_s + 2d_{z,N_z+1/2}} (c_{i,N} - c_a).
\end{aligned}
\tag{16}
$$

  - interface under the patch: for $i \leq i_P$:

$$F_{i,1/2} = F_{i,N_z+1/2} = 0, \ j = 1, \ldots, N_z. \tag{17}$$

In the above formulae, $d_{r,i+1/2}$ and $d_{z,j+1/2}$ represent some mean value of d_r and d_z over the corresponding interface.

THEOREM 4.2 (WELL POSEDNESS OF THE DISCRETE SYSTEM) Let $\mathcal{M}$ be defined in Definition 4.1, there exists a unique solution $(c_{i,j})_{\substack{i=1,\ldots,N_r \\ j=1,\ldots,N_z}}$ to the system (12)-(17). Furthermore, one has:

$$c^* \leq c_{i,j} \leq c_a, \ \forall i = 0, \ldots, N_r, \ \forall j = 1, \ldots, N_z. \tag{18}$$

Proof First note that if $f = 0$, $c_a = 0$, then the system (12)-(17) admits 0 as a unique solution, which shows that for any c_a, if f does not depend on c, then the system (12)-(17) admits a unique solution. There remains to prove the existence and uniqueness in the nonlinear case. As in the continuous case (see Theorem 3.2), the uniqueness of the solution is an easy consequence of the fact that f is negative. Existence of a solution follows from Brouwer's fixed point theorem. Indeed, one considers the mapping T from $\mathbb{R}^N$ to $\mathbb{R}^N$, defined by $T(\tilde{c}) = c$, where c is the unique solution of the linearised problem obtained from (12)–(17) when replacing $f(c_{i,j})=$ by $f(\tilde{c}_{i,j})$ in the right hand side of (12). Indeed, it was shown in [8] that for such a linear system, one may obtain an estimate in the L^2 norm on the approximate solution (Proposition 5.1 of [8]), which only depends on the data. Hence we deduce that T maps $L^2(\Omega)$ onto a closed ball, and Brouwer's theorem [2] applies.

Let us finally remark that (18) is easily deduced by using the assumptions of f (see Definition 3.1) and the fact that $c_a \geq c^*$, where the compensation point c^* is defined in (3). □

THEOREM 4.3 (CONVERGENCE OF THE FINITE VOLUME SCHEME) Let $\mathcal{M} = (K_{i,j})_{\substack{i=1,...,N_r \\ j=1,...,N_z}}$ be defined in Definition 4.1, and $(c_{i,j})_{\substack{i=1,...,N_r \\ j=1,...,N_z}}$ be the unique solution to 12–17. Let $c_{\mathcal{M}} \in L^2(\Omega)$ be the piecewise constant solution defined a.e. by:

$$c_{\mathcal{M}}(x) = c_{i,j}, \forall x \in K_{i,j}. \tag{19}$$

Then $c_{\mathcal{M}}$ converges in $L^2(\Omega)$ to the unique solution c of (9), as $h_{\mathcal{M}}$ tends to 0.

Proof The proof of this result uses suitable adaptations to the cylindrical diffusion operator considered here, of the tools developed in [4] for a semilinear problems with Dirichlet boundary condition and in [8] for linear convection diffusion problems with Robin boundary conditions. The first main adaptation concerns the proof of discrete Poincaré (Lemma 4.3 of [8]), which in fact is simpler in the case of the axisymmetric meshes which are considered here. The other adaptation concerns the passage to the limit in the scheme. In [4], the convergence of the scheme was proven for a more general semi linear problem, but with Dirichlet boundary conditions. Here we consider Robin boundary conditions, so the treatment of the boundary is somewhat different. Indeed, we consider a sequence of approximate solutions $(c_{\mathcal{M}}, c_\Gamma)$, where c_Γ is a piecewise constant function from $\partial\Omega$ to $\mathbb{R}$ such that the constant value c_σ of c_Γ on a given edge σ included in $\partial\Omega$ is determined by equalling the numerical flux (given by (15)–(17)) to $\frac{\Sigma}{d}(c_K - c_\sigma)$, where Σ is the area of σ, K the control volume to which σ is boundary, d the distance between the center point fo K and σ, and c_K the unknown associated to K. Now, using the same technique as that of the proof of Theorem 2 in [4] yields that the limit $(\widetilde{c}, \overline{c})$ sequence of approximations $(c_{\mathcal{M}}, c_\Gamma)$ as the mesh size tends to 0 (which exists thanks to a compactness result obtained from an estimate on the translate and Kolmogorov's theorem, see [5] or [4]) satisfies :

$$\int_\Omega \widetilde{c}(x)\, \nabla \cdot (D(x)\nabla\varphi(x))dx + \int_{\partial\Omega} D(x)\nabla\varphi(x) \cdot \mathbf{n}(x)(\overline{c}(x) - c_a)d\gamma(x) = \int f(\widetilde{c}(x), x)\varphi(x)dx,$$

for all function $\varphi \in C^1(\Omega)$ such that $\varphi = 0$ on $\partial\Omega$. Using the following lemma yields that $\widetilde{c}$ is in fact the unit solution of (9), which concludes the proof.

LEMMA 4.4 let Ω be an open bounded subset of $\mathbb{R}^d$, $d \geq 1$, with Lipschitz boundary. Let $f \in L^2(\Omega), v \in L^2(\partial\Omega)$, $a \in C^\infty(\bar{\Omega})$ such that $a \geq \underline{a} > 0$ and assume that

$$\int_\Omega u(x)\text{div}(a(x)\nabla\varphi(x)d(x) + \int_{\partial\Omega} a(x)\nabla\varphi(x) \cdot \mathbf{n}(x)v(x)d\gamma(x) = \int f(x)\varphi(x)dx,$$

for all functions $\varphi \in C^1(\Omega)$ such that $\varphi = 0$ on $\partial\Omega$; then $-\text{div}(a\nabla u) = f$ in Ω and $\gamma(u) = v$ on $\partial\Omega$, where γ denotes the trace operator from $H^1(\Omega)$ to $L^2(\Omega)$.

$\square$

5 Numerical solution of the discrete problem

The scheme (12)–(17) may then be written as:

$$MC = b(C), \tag{20}$$

where:

- M is a symmetric positive definite matrix and $b(C) \in \mathbb{R}^N$, with $N = N_r \times N_z$. It is easily shown that M satisfies the following discrete positive property:

$$Mx \geq 0 \Longrightarrow x \geq 0. \tag{21}$$

- $C \in \mathbb{R}^N$ is a vector of $\mathbb{R}^N$ with components c_k (the unknowns of the system), $k = 1, \ldots, N$,

- b is a (component wise) non increasing function from $\mathbb{R}^N$ to $\mathbb{R}^N$.

Let us first remark that since the matrix M is symmetric definite positive, and since b is continuous and non increasing function, one may show that there exists a unique solution to (20). In order to solve this nonlinear system, one could use Newton's method, which has the advantage of converging fast: the method is known to be locally convergent with a quadratic convergence if sufficient regularity conditions are fulfilled. However, it is also well known that Newton's method may not converge at all if the initial guess is taken too far from the solution of the equation. Hence we prefer to choose a more robust (even though slower) method, based on the monotony of the constructed sequence of approximations. In order to apply a monotonic fixed point method and prove its convergence we need to apply it to a system of the form $Bx = g(x)$ where g is a non decreasing continuous function and where the matrix B satisfies the discrete maximum principle, that is if $x \in \mathbb{R}^N$ is such that $Bx \geq 0$, then $x \geq 0$ (see [9] for further details). Note that this last property is important when discretizing diffusion systems, since this ensures that the approximate molar fractions will remain positive.

It is easily seen that the functions b_k (components of b) are continuous and non increasing. However, the functions g_k defined by $g_k(x) = b_k(x) + \omega x$ with $\omega = \frac{Vc_{max}}{K_c}$ is non decreasing (because in fact, $-\omega$ is a lower bound of the derivative of b_k when it is derivable). Hence we shall apply the monotonic fixed point method of [9] to the "relaxed" system

$$MC + \omega C = b(C) + \omega C.$$

It is easily shown that the matrix $M + \omega Id$ (where Id denotes the identity matrix) still satisfies the discrete maximum principle and that the function g is now non decreasing. Furthermore the other assumptions which are needed to prove the convergence of the method (namely that 0 is a sub solution of the system and there exists a positive super solution of the system, see [9]) are easily shown to be satisfied. Hence, the sequence $(C^{(k)})_{k \in \mathbb{N}} \subset \mathbb{R}^N$ defined by:

- $C^{(0)} \in \mathbb{R}^N$ chosen arbitrarily (or rather, adequately...)

- for $k \geq 0$, $C^{(k+1)} \in \mathbb{R}^N$ is the unique solution to the following linear system:

$$MC^{(k+1)} + \omega C^{(k+1)} = F(C^{(k)}) + \omega C^{(k)}$$

converges to the unique solution of (20) (which is also the unique solution to (12)–(17) (see [9]). Indeed, we use this algorithm to solve the discrete nonlinear system, and the convergence up to a tolerance of 10^{-6} on the relative error is found in less than 10 iterations with the given parameters.

6 Estimation of $D(= D_{CO_2})$:

In the biological application (see [12]) we are mainly interested in the role of lateral diffusion, we therefore choose to implement our method according to this objective. Indeed, we integrate the 3D diffusion equation over the depth of the leaf (which is the z direction), and obtain a 2D diffusion equation, the unknown of which is the averaged value of the concentration over the depth of the leaf. Let us give some details; integrating Eq. (5) in the z direction yields :

$$\int_0^H -\nabla_{xy} \cdot (D\nabla c) \ dz - D\nabla c \cdot \mathbf{n}(H) + D\nabla c \cdot \mathbf{n}(0) = \int_0^H f(c)dz \qquad (22)$$

where $\nabla_{xy}\cdot$ denotes the two dimensional divergence operator. Let us the denote by $\widetilde{c}$ the mean value of c in the z direction. In equation (22), we approximate $\int_0^H D\nabla c \ dz$ by $H\widetilde{D}\nabla\widetilde{c}$, where $\widetilde{D}$ denotes the mean value of D in the z direction (note that the third component of the vector $\nabla\widetilde{c}$ is zero); we also approximate the source term $\int_0^H f(c)dz$ by $Hf(\widetilde{c})$. Furthermore, we take into account the boundary conditions (7), also approximating the point wise values $c(H)$ and $c(0)$ by $\widetilde{c}$. We then obtain the following 2D model:

$$\nabla_{xy} \cdot (\widetilde{D}\nabla\widetilde{c}) + \frac{g_s}{H}(\widetilde{c} - c_a) = f(\widetilde{c}) \qquad (23)$$

This equation has to be discretized on a disk of radius R. Since the diffusion coefficient is constant in the r and θ directions, the axisymmetric finite volume discretization presented in the above section boils down to a one dimensional computation (see [7]) in the sequel we shall denote by D the mean value in the z direction of the lateral coefficient (which was denoted by d_ℓ in (8)).

Determination of the lateral diffusion coefficient In the above section, we devised a method to compute the internal concentration of CO_2, given the assimilation parameters, the conductance g_s, the atmospheric CO_2 concentration c_a, and the diffusion parameter D within the leaf. Now, as we mentioned in the introduction, the diffusion coefficient within the leaf is not well known. We shall therefore determine this parameter by fitting the experimental data with the results from the model at different D, and choose the parameter which minimises the least square function defined by the computed values and the experimental values. The model produces a string of c values. In order to compare this profile with the experimental data we extract two transects perpendicular to each other centred in the center of the patch. Since we choose the size of a discretization cell in the model equal to that of the measurement cell, the calculated and estimated values of c may be easily compared cell by cell from the center of the patch.

To determine the coefficient of lateral diffusion we compare the theoretical curve with the experimental data varying the coefficient of diffusion. For a particular determination of D on a given experiment numbered k, we calculated the mean punctual relative error, ε_k^m, between the experimental data, c^k, and the calculated c^t. This error is defined by: $\varepsilon_k^m = \frac{1}{n}\sum_{i=1}^n \frac{|c_i^t - c_i^k|}{|c_i^k|}$. where n is the number of measured values of c_i^k on the transect. The smallest relative errors $((\varepsilon_k^m)^{min})$ gives the best estimation of the lateral diffusion coefficient. We then define the mean relative error $\mu_m = \frac{\sum_{k=1}^K (\varepsilon_k^m)^{min}}{K}$ where K is the number of experimental measurements performed for each species. The standard deviation of the parameter D around its mean $D_{CO_2}^m$ is given by $\sigma = \sqrt{\frac{\sum_{k=1}^K (D^k - D^m)^2}{K}}$
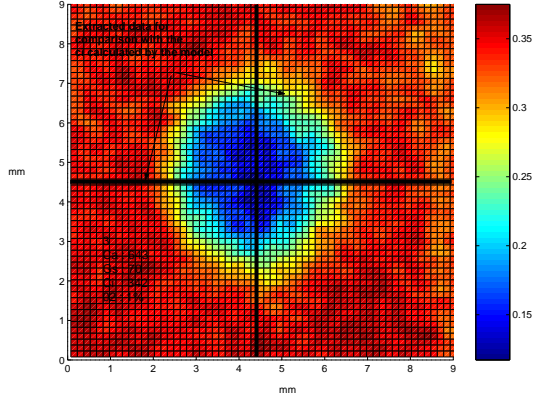
Image of a leaf portion with a patched area. the distance in mm are distances from an arbitrary point. Each square corresponds to a measure of c (here the scale refers to the fluorescence parameter $\frac{fq}{fm'}$ which is linked to c). The black line indicates the extracted values to compare with the profile calculated with the model.

Figure 3: Measured internal concentrations of CO_2

Sensitivity analysis We analysed the sensitivity of the estimated D given by the model to various parameters X. Variation of X are given as a percentage of the initial value X_0 and variation in D are given as a percentage of initial D. To analyse the sensitivity of the profile to the parameter X, the variation of the profile are given as a percentage of the mean punctual differences between the new profile P_{X_0} and the initial profile $P_{X+\delta X}$ define by $V = \frac{1}{n} \sum_{i=1}^{n} \frac{|c_i^{X_0} - c^{X+\delta X}|}{|c_i^{X_0}|}$. The elasticity of the parameter or the profile P relative to the parameter X is given by $e = V/\frac{\delta X}{X_0}$.
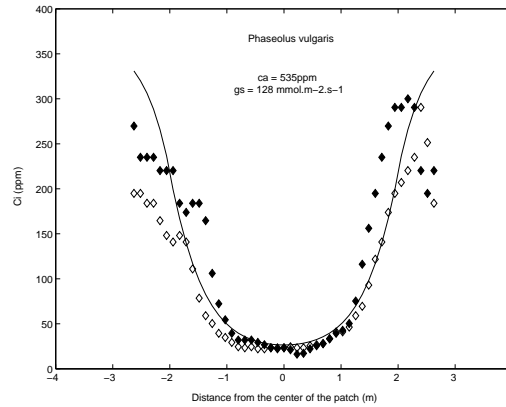

Figure 4: Experimental and calculated profiles for *Phaseolus vulgaris*. The dotted lines represent c values from experimental measurements for two perpendicular transects across the patch, the solid line is the profile calculated with the model, using the D given by the best fit with the experimental data. The patch radius is equal to $2mm$. External CO_2 molar fraction, c_a, and stomatal conductance, gs, are the values given by gas exchange measurements.

Results Figure 4 illustrates typical results obtained. One may observe that towards high c_a, outside the patch, the calculated profile deviates from the experimental data. There are essen-

tially two reasons: firstly there are veins in the mesophyll tissues that punctually disturb the determination of c, secondly at high c, around $300ppm$, the limit of the experimental determination of c is reached. The corresponding computed lateral diffusion coefficient for *Phaseolus vulgaris*, D_{CO_2}, is equal to $73\mu mol\ m^{-1}\ s^{-1}$. D_{CO_2} may also be expressed as a percentage of the diffusion coefficient in free air ($D_{CO_2}^{fa} = 1.51\ 10^{-5}\ m^2\ s^{-1}$ or $617\mu mol\ m^{-1}\ s^{-1}$ at 101.3 kPa and $20°C$). Since the reduction is mainly due to the anatomy of the leaf, especially the porosity of the medium and the tortuosity of the pathways, the % of reduction also gives an insight on the anatomy of the leaf. Here $D_{CO_2} = 12.4\% D_{CO_2}^{fa}$. Measurements were performed on 5 different leaves of *Phaseolus vulgaris* An average of five measurements, each at different external CO_2 molar fraction, is performed for every leaf. The standard deviation, equals to 1.8 $\% D_{CO_2}^{fa}$, partly reflects biological variability. Measurements were made on 5 different leaves thus the areas investigated do not have identical anatomy. The mean punctual relative error, μ_m, between the experimental data and the model is around 25%. As well as reflecting experimental variation, this error can be explained by the lack of precision of the fit in the R dimension due the measurements and discretization precisions. Indeed the radius of the experimental patch can vary by 0.1mm and the center, or border of the patch, do not necessarily match with the center of a measurement cell. The accuracy of the computed value for D_{CO_2} depends on the reliability of the other biological parameters. The principal source of error in the model arises from the assimilation parameters. In particular the thickness of the photosynthesising tissue is not precisely known, and therefore neither is the sink strength. We are currently working to improve the photosynthesis and anatomical data in order to use the full 3D discretization, which would lead to a better estimation of D_{CO_2}. Secondly it is interesting to note that the elasticity of the theoretical profile to different D_{CO_2} is relatively low, 0.37 for *Phaseolus vulgaris*. This low sensitivity is itself an important result. Indeed it suggests that CO_2 depletion with the assimilation parameters considered here is mainly driven by consumption. It is worth noting that the sensitivity of the profile to D_{CO_2} depends on the assimilation strength. If assimilation is low, sensitivity to D_{CO_2} will be high. Similarly sensitivity of the profile to the assimilation strength depends on D_{CO_2}. The higher D_{CO2} the higher the sensitivity to assimilation strength. Recently Pieruschka et al. [17] also calculated a lateral diffusion coefficient for *Phaseolus vulgaris* using a different method and they found it to be nearly zero. This is not compatible with the results of our experiments; since all c under the patch are not equal to the compensation point c^* there must be some diffusion.

7 Perspectives

We used the finite volume method for the simulation of the diffusion of CO_2 through the leaf tissue, using an axisymmetric geometry. Numerical tests were performed and allowed us to derive from experimental data the rate of lateral diffusion within the leaf tissue. The interest of this work is two-fold: from the point of view of numerical analysis, it shows that the finite volume method with cylindrical meshes works quite well, and that convergence and error estimate results which were obtained for polyhedral meshes may be extended to this type of mesh. From the biological point of view, we were able to infer that the diffusion process is not sufficient with respect to assimilation to supply enough CO_2 under the patch. Hence, under moderate to high light, if stomata close in patches, the photosynthesis will be affected regardless of the anatomy of the leaf.

Future research requires a more precise study of the porous media itself, and "real" axi-symmetric tests in order to see the influence of the depth of the leaf tissue. One needs to find a law in particular for the variation of D_{CO_2} in z. Another interesting problem to solve mathematically is the sensitivity of the profile to D_{CO_2} as a function of the assimilation strength and reciprocally the sensitivity of the gradient to assimilation strength as a function of D_{CO_2}. Future experimental measurements should be conducted for the same species with different sink strength, this can be achieved by modifying Rubisco content or its affinity to CO_2. On the one hand these experiments are necessary to verify that the estimated D_{CO_2} by the model is independent of assimilation rate, which it should be. On the other hand it will provide experimental data to test sensitivity of the gradient to the assimilation strength for a given D_{CO_2}.

References

[1] Aalto T., Vesala T., Mattila T., Simbierowicz P., Haris P,. (1999) A three-dimensional stomatal CO_2 exchange model including gaseous phase and leaf mesophyll separated by ireedular interface. J. Theor. Biol., 196, 115-128.

[2] Deimling, K. (1980), *Nonlinear Functional Analysis*, (Springer, New York).

[3] Evans J.R., von Caemmerer S.C. (1996) Carbon dioxide diffusion inside leaves. Plant Physiol 110: 339-346

[4] Eymard, R., Gallouët T. and Herbin R. (1999), Convergence of finite volume approximations to the solutions of semilinear convection diffusion reaction equations, Numer. Math., 82, 91-116.

[5] Eymard R., Gallouët T., Herbin R. (2000) The finite volume method. In Ph. Ciarlet and J.L. Lions, eds, Handbook for Numerical Analysis, Vol. VII. North Holland, pp 715-1022

[6] Farquhar G.D., von Caemmerer S., Berry J.A.(1980), A biochemical model of photosynthetic CO_2 assimilation in leaves of C_3 species. Planta 149, 78-90.

[7] Gallouët E. (2004), Diffusion of CO2 in leaves, MSc thesis, Université de Paris 11, 49 pp.

[8] Gallouët, T., Herbin R. and Vignal M.H., (2000), Error estimate for the approximate finite volume solutions of convection diffusion equations with general boundary conditions, *SIAM J. Numer. Anal.*, 37, 6, 1935-1972.

[9] Herbin R. (2004) *Cours d'analyse numérique*, Centre de Mathématiques et Informatique, Université de Provence, Marseille, `http://www.cmi.univ-mrs.fr/~herbin/PUBLI/polyananum.pdf`

[10] Lawson T., Weyers J., At'Brook R. (1998), The nature of heterogeneity in the stomatal behaviour of Phaseolus vulgaris L. primary leaves, *J. Exp. Bot.* 49: 1387-1395.

[11] Meyer S Genty B (1998) Mapping intercellular CO2 mole fraction (Ci) in Rosa rubiginosa leaves fed with abscisic acid by using chlorophyll fluorescence imaging: significance of Ci estimated from leaf gas exchange. *Plant. Physiol.*, 116: 947–957.

[12] Morison J., Gallouët E., Lawson T., Cornic G., Herbin R., Baker N. (2005) Lateral diffusion in leaves is not sufficient to support photosynthesis, submitted, March 2005.

[13] Nobel P. S., (1991), Physiochemical and environmental plant physiology, Acad. Press, San Diego, 635pp.

[14] Pachepsky L.B., Acock B. (1996) A model 2DLEAF of leaf gas exchange: development, validation, and ecological application, *Ecol. Modelling* 93: 1-18.

[15] Parkhurst D.F. (1986) Internal leaf structure: a 3-dimensional perspective. In Givnish TJ, ed. *On the economy of plant form and function*, Cambridge Univ Press, NY, pp 215-249

[16] Parkhurst D.F. (1994), Tansley Review 65: Diffusion of CO2 and other gases inside leaves, *New Phytol.* 126: 449–479

[17] Pieruschka R., Schurr U., Jahnke S. (2005), Lateral gas diffusion inside leaves. *J. Exp. Bot.* 56: 857–864.

[18] Terashima I. (1992), Anatomy of non-uniform photosynthesis, *Photosynth. Res.* 31: 195–212.